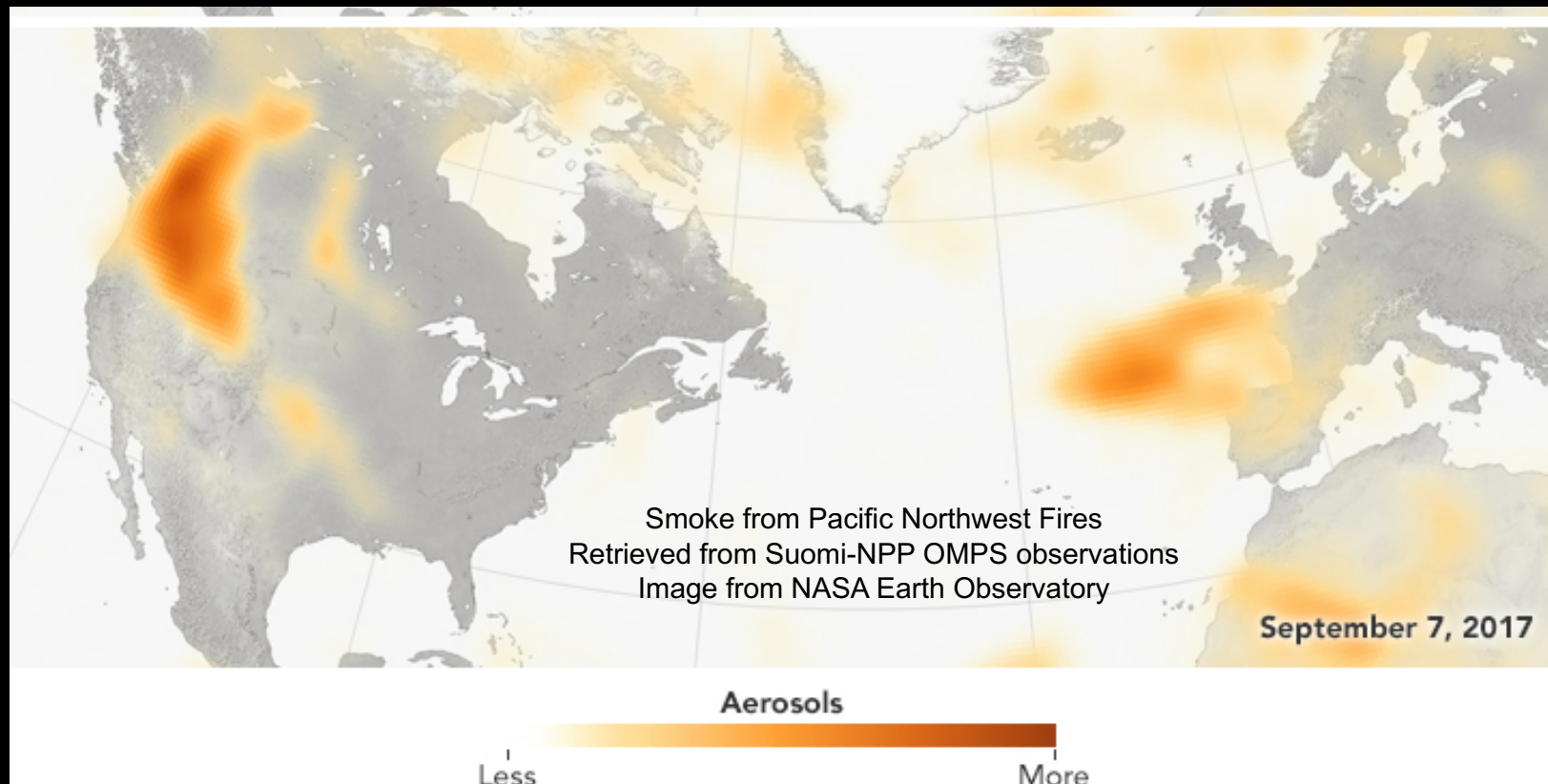


# Potential of satellite spectral solar irradiance (SSI) measurements in ground-based remote sensing of atmospheric aerosols and trace gases

Charles Ichoku<sup>1</sup>, Jae Lee<sup>1,2</sup>, Dong Wu<sup>1</sup>, Alexander Smirnov<sup>1,3</sup>, and Nader Abuhassan<sup>1,2</sup>

1. NASA Goddard Space Flight Center, Greenbelt, Maryland, USA.
2. JCET, University of Maryland, Baltimore County, Maryland, USA.
3. Science Systems and Applications Inc. (SSAI), Lanham, Maryland, USA.



Presented at the 2018 Sun-Climate Symposium, Lake Arrowhead, California, March 19-23, 2018

# 2017 Decadal Survey Recommended NASA Priorities

## Designated

### Categories



### Designated

### Earth System Explorer

### Incubation

### Venture

TARGETED OBSERVABLE	SCIENCE/APPLICATIONS SUMMARY	CANDIDATE MEASUREMENT APPROACH	Designated	Explorer	Incubation
<b>Aerosols</b>	<b>Aerosol properties, aerosol vertical profiles, and cloud properties</b> to understand their direct and indirect effects on climate and air quality	Backscatter lidar and multi-channel/multi-angle/polarization imaging radiometer flown together on the same platform	X		
<b>Clouds, Convection, &amp; Precipitation</b>	<b>Coupled cloud-precipitation state and dynamics</b> for monitoring global hydrological cycle and understanding contributing processes	Radar(s), with multi-frequency passive microwave and sub-mm radiometer	X		
<b>Mass Change</b>	<b>Large-scale Earth dynamics</b> measured by the changing mass distribution within and between the Earth's atmosphere, oceans, ground water, and ice sheets	Spacecraft ranging measurement of gravity anomaly	X		
<b>Surface Biology &amp; Geology</b>	<b>Earth surface geology and biology</b> , ground/water temperature, snow reflectivity, active geologic processes, vegetation traits and algal biomass	Hyperspectral imagery in the visible and shortwave infrared, multi- or hyperspectral imagery in the thermal IR	X		
<b>Surface Deformation &amp; Change</b>	<b>Earth surface dynamics</b> from earthquakes and landslides to ice sheets and permafrost	Interferometric Synthetic Aperture Radar (InSAR) with ionospheric correction	X		

# Outline

- Aerosol retrieval from satellite observations
- Ground-based Aerosol remote sensing using sun photometers
- Calibration of sun photometers and relationship to SSI
- The need to use satellite SSI for ground instrument calibration
- Conclusions

# Basic Concepts of Satellite Aerosol Retrieval Algorithms

$$\rho^{\text{toa}}_{\lambda} \sim \rho^{\text{surf}}_{\lambda} + \rho^{\text{atm}}_{\lambda}$$

Where,  $\rho^{\text{toa}}_{\lambda}$  is the spectral reflectance measured at the top of the atmosphere (TOA)

$\rho^{\text{surf}}_{\lambda}$  is the component of the TOA reflectance contributed by the surface

$\rho^{\text{atm}}_{\lambda}$  is the component of the TOA reflectance from the atmosphere (or path radiance)

➤ Over ocean,  $\rho^{\text{surf}}_{\lambda}$  is known (550-2130nm)

- $\rho^{\text{atm}}_{\lambda} \sim \tau_{\lambda} * P_{\lambda}(\theta)$ ; the spectral information can be used to derive information on aerosol type, which is then used to derive the aerosol loading.

➤ Over land,  $\rho^{\text{surf}}_{\lambda}$  is complex

- if  $\rho^{\text{atm}}_{\lambda=2.1} \sim 0$ , then  $\rho^{\text{surf}}_{\lambda=2.1}$  can be estimated
- if  $\rho^{\text{surf}}_{\lambda} \sim f(\rho^{\text{surf}}_{\lambda=2.1})$  then  $\rho^{\text{atm}}_{\lambda}$  can be derived
- $\tau_{\lambda}$  can be derived assuming an aerosol model, i.e  $P_{\lambda}(\theta)$ ; if there are relationships between the spectral reflectances at different wavelengths.

Dubovik et al., 2002, JAS paper on aerosol optical properties (p. 591):

Modeling the aerosol effects on atmospheric radiation, by solving the radiative transfer equation, requires the following aerosol optical properties:

- aerosol optical thickness  $\tau_\lambda$  (loading);
- phase function  $P(\Theta; \lambda)$  (angular dependence of light scattering),
- single-scattering albedo  $\omega_{0\lambda}$  (ratio of scattering to scattering + absorption).

## Sayer et al., 2016, JGR, Extending Deep Blue aerosol retrieval

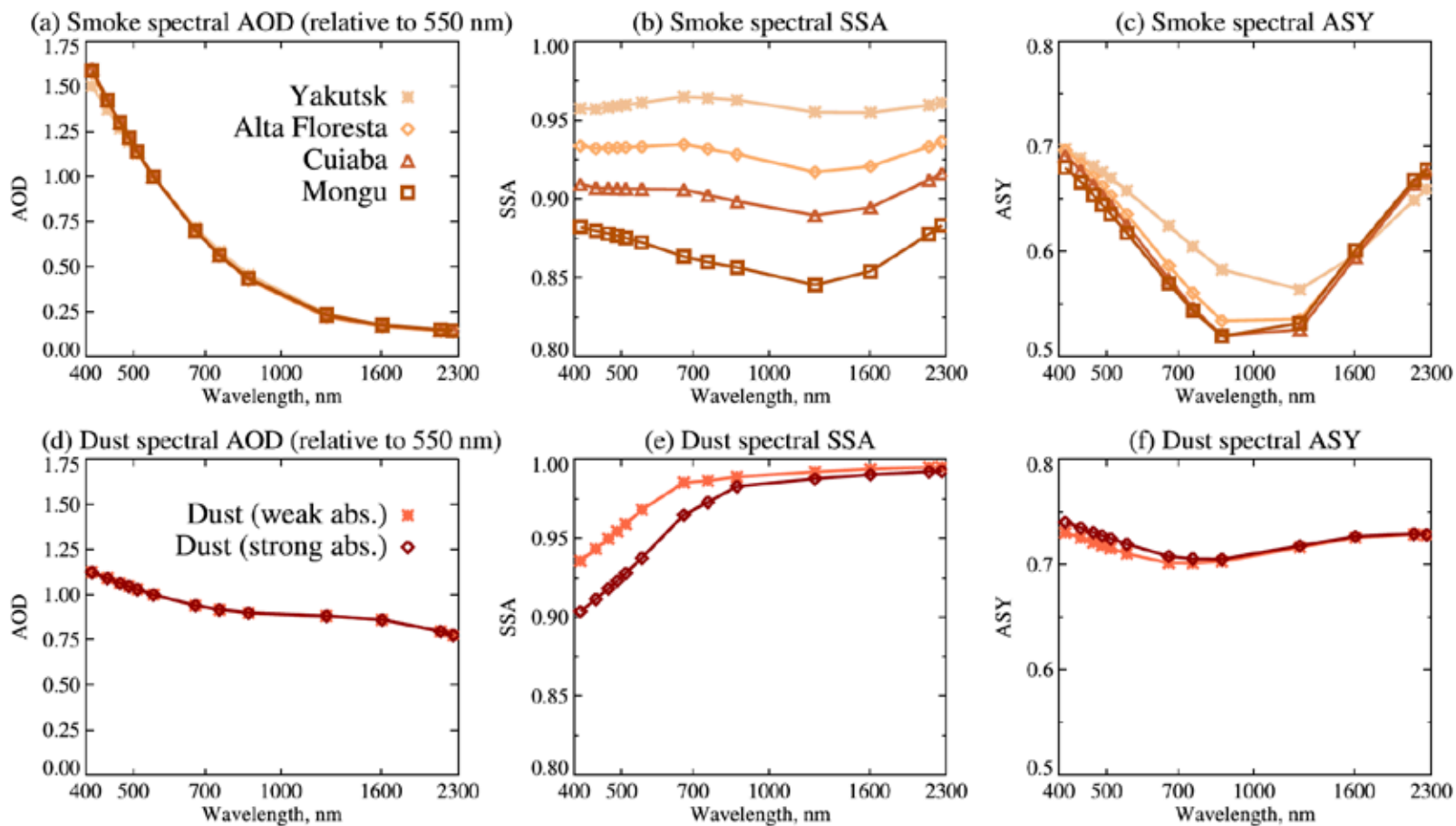
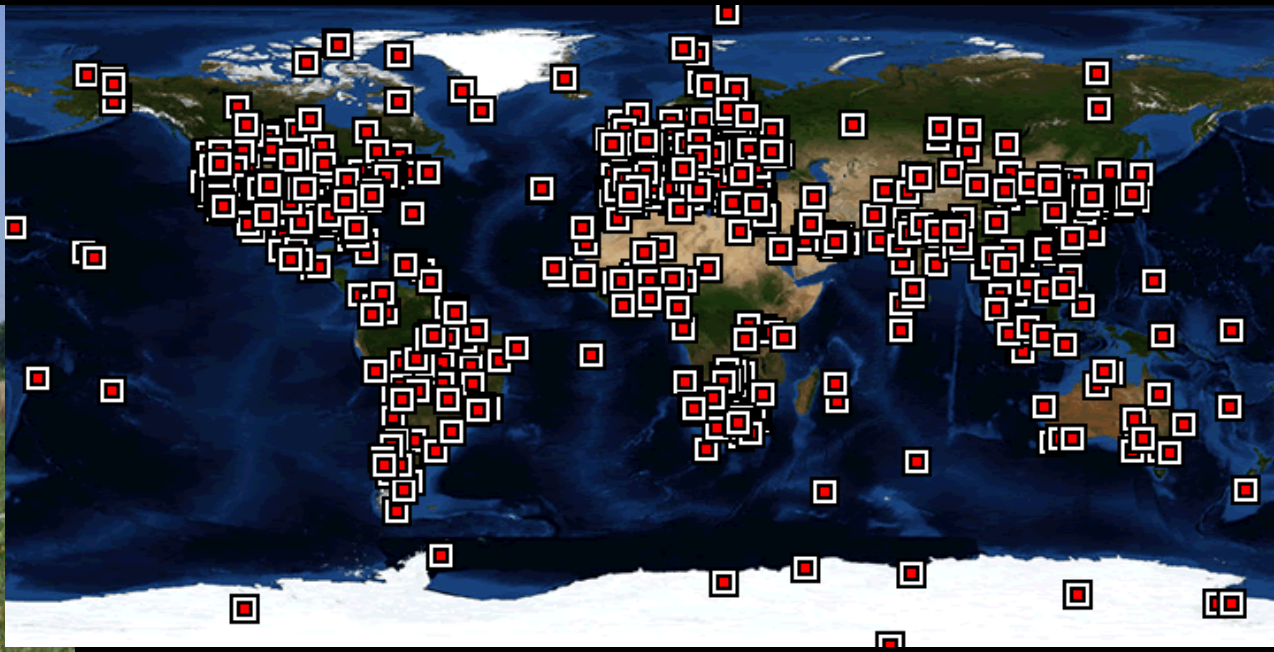


**Figure 3.** Summary of spectral optical properties of the (a–c) four smoke and (d–f) two dust aerosol optical models studied. Panels show spectral AOD (Figures 3a and 3c), spectral SSA (Figures 3b and 3e), and spectral ASY (Figures 3c and 3f). Paler to stronger colors are used to indicate models with weaker to stronger levels of absorption.

# Summary of satellite aerosol retrieval

Models used for aerosol retrieval from satellite observations are often based on aerosol measurements from the ground, predominantly the Aerosol Robotic Network (AERONET) of ground-based sun photometers/sky radiometers. These models are often used to develop look-up tables (LUT) to facilitate aerosol retrieval.

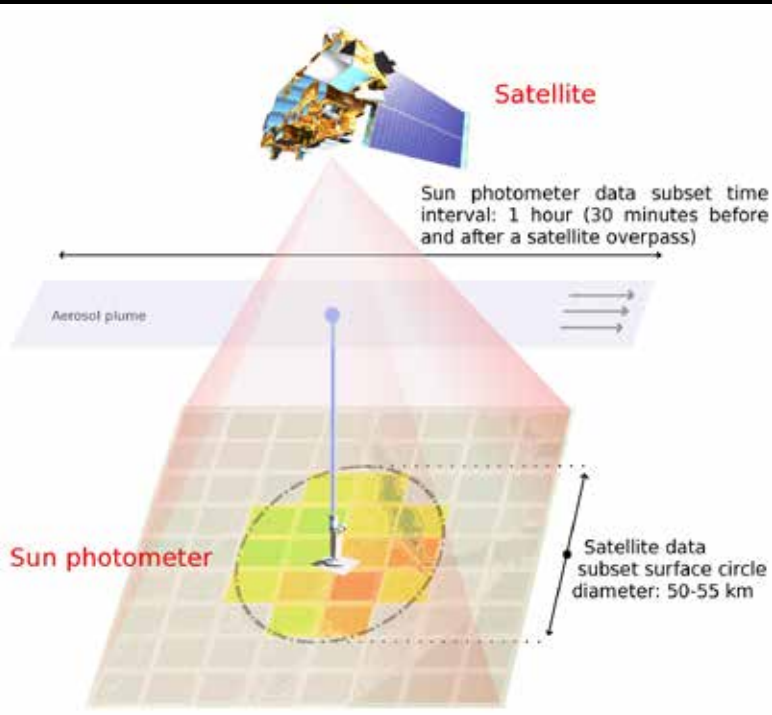
# Ground-based aerosol remote sensing based on direct spectral solar irradiance: AERONET example



<https://aeronet.gsfc.nasa.gov>

# Ground-based AERONET used to validate satellite aerosol retrieval

MAPSS (Multi-sensor Aerosol Products Sampling System) <http://giovanni.gsfc.nasa.gov/mapss/>



### MAPSS: Multi-sensor Aerosol Products Sampling System

This user interface is used to obtain selected parameter statistics from the MAPSS database for a chosen location and time period. Time Series Plot is the available service. Plot output is rendered as a graph and is also available in ASCII format.

**Data Selection**  **NOW**

**Plot Data**

**Select Station**

**Select Plot**  
Satellite Collocated with AERONET  
 Time Series  
 Scatter Plot

**Select Measurements**  
Click each cell above displaying with the software that is how many of this qualified measurements. Select a measurement and then click 'Add' those to additional measurements.  
 Basic  Advanced

Product	Parameter	Layer	Measurement
AERONET aerosols L2, ver. 2			
AERONET discrimination L2, ver. 41			
AERONET inversions L2, ver. 2			
AERONET inversions L2, ver. 2			
CALIPSO 3D volume rate layer aerosols L2, ver. 3			
More...			<input type="button" value="Add"/>

**Selected Measurements**

**Select Date Range**  
 Date Picker  Seasonal Search

Format: YYYY-MM-DD    MM/Range: 1979-01-01 to 2015-10-01

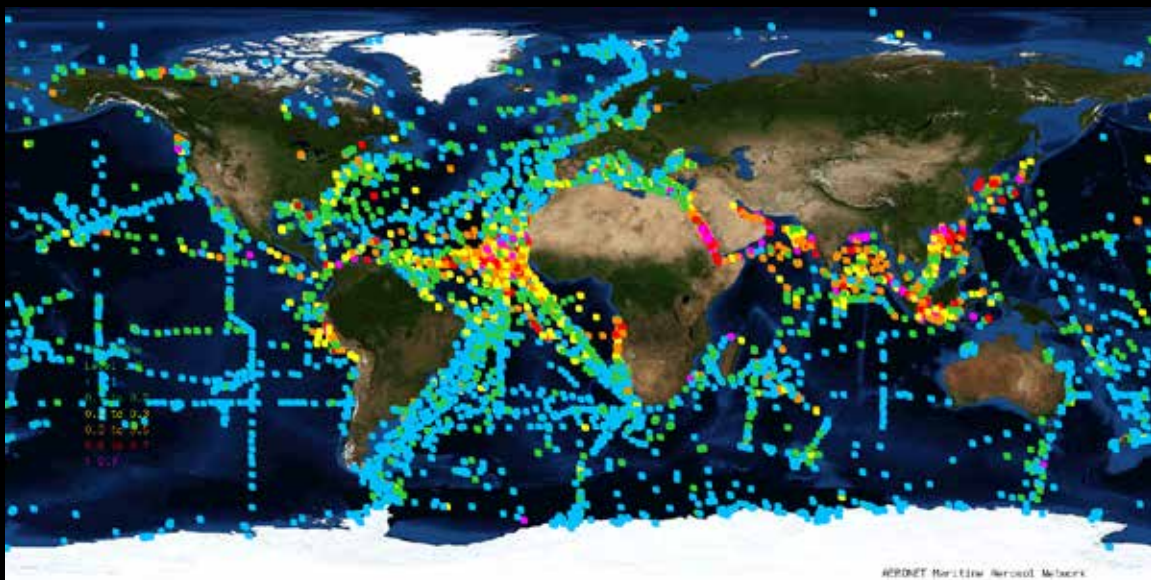
Date Range (UTC):  to

**Plot Data**

AERONET, MODIS, MISR, OMI, POLDER, CALIOP, SeaWiFS, VIIRS

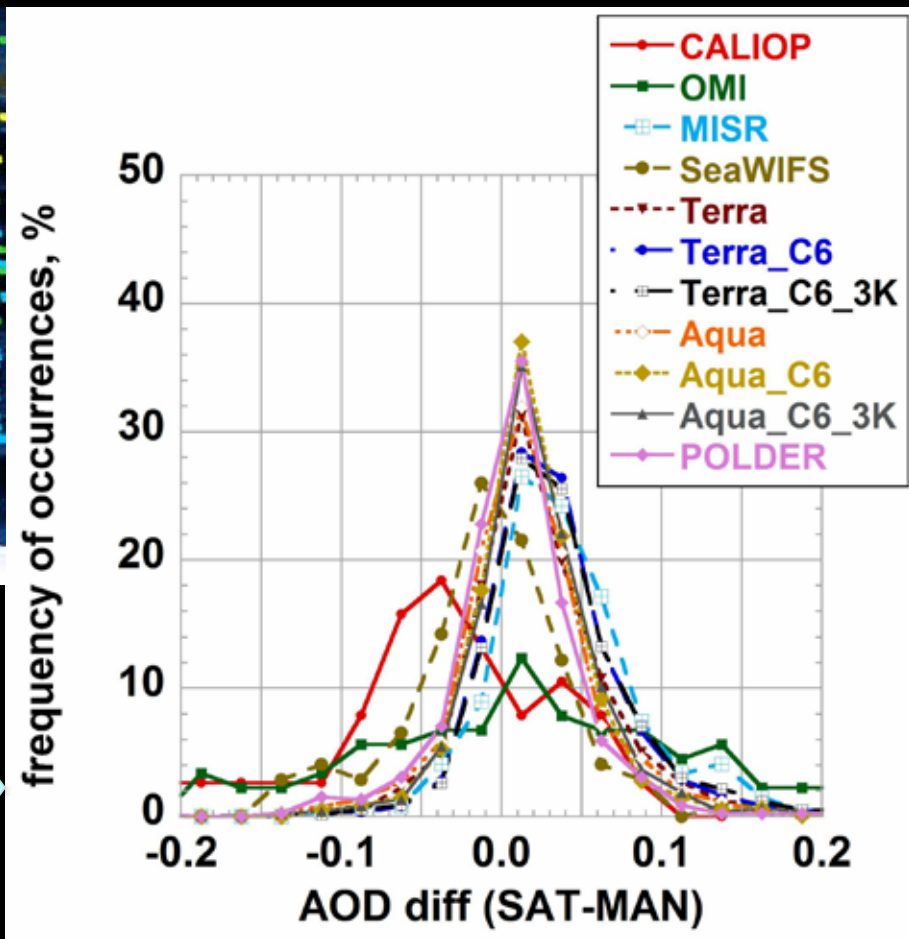
Petrenko et al., 2012, AMT; Petrenko and Ichoku, 2013, ACP

# Ship-based MAN used to validate satellite aerosol retrieval



Microtops II  
Sun photometer

Frequency distributions of aerosol optical depth (AOD) differences between various satellite sensors and sun-photometer.



Smirnov et al., 2017, SPIE

## Aerosol remote sensing based on Beer-Bouguer-Lambert's law. Simply:

Where,

$$I(\lambda) = I_0(\lambda) \exp[-\tau(\lambda)/\cos\theta]$$

$I_0(\lambda)$  is the extraterrestrial flux at wavelength  $\lambda$ ,

$I(\lambda)$  is the flux reaching the ground,  $\theta$  is the solar zenith angle, and

$\tau(\lambda)$  is the total optical depth

### **Dutton et al., 1994, JGR states:**

**“The need for absolute irradiance measurements is eliminated for  $\tau(\lambda)$  computation because the linear response of the sunphotometer is such that a linear conversion constant cancels from both sides of the equation, and the instrument output voltages,  $V(\lambda)$  and  $V_0(\lambda)$  replace  $I(\lambda)$  and  $I_0(\lambda)$ .”**

**This means:**  $V(\lambda) = k * I(\lambda)$  and  $V_0(\lambda) = k * I_0(\lambda)$

Where  $k$  is a convolution of various instrument specific parameters (filter transmission, field of view, detector sensitivity, etc.)

**Thus, for direct sun measurement using sun photometers:**

$$V_{\lambda} = V_{0\lambda} D^{-2} \exp(-\tau_{\lambda} M)$$

$$V_w = V_{0w} D^{-2} \exp[-\tau_w M - k(WM)^b]$$

where, for each channel (wavelength  $\lambda$  in microns),

$V_{\lambda}$  = the signal measured by the instrument at wavelength  $\lambda$ ,

$V_{0\lambda}$  = the extraterrestrial signal at wavelength  $\lambda$ ,

$D$  = Earth-Sun Distance in Astronomical units at time of observation,

$\tau_{\lambda}$  = total optical thickness ( $\tau_{\lambda} = \tau_{a\lambda} + \tau_{R\lambda} + \tau_{O3\lambda}$ ) at wavelength  $\lambda$ ,

$\tau_{a\lambda}$  = aerosol optical thickness (AOT) at wavelength  $\lambda$ ,

$\tau_{R\lambda}$  = Rayleigh (air) optical thickness at wavelength  $\lambda$ ,

$\tau_{O3\lambda}$  = Ozone optical thickness at wavelength  $\lambda$ ,

$M$  = the optical air mass

$W$  = vertical water vapor column thickness

$k$  and  $b$  are instrument constants numerically derived for the 936 nm filter.

## Sun-photometer calibration approaches:

Langley calibration under pristine conditions (Mauna Loa)

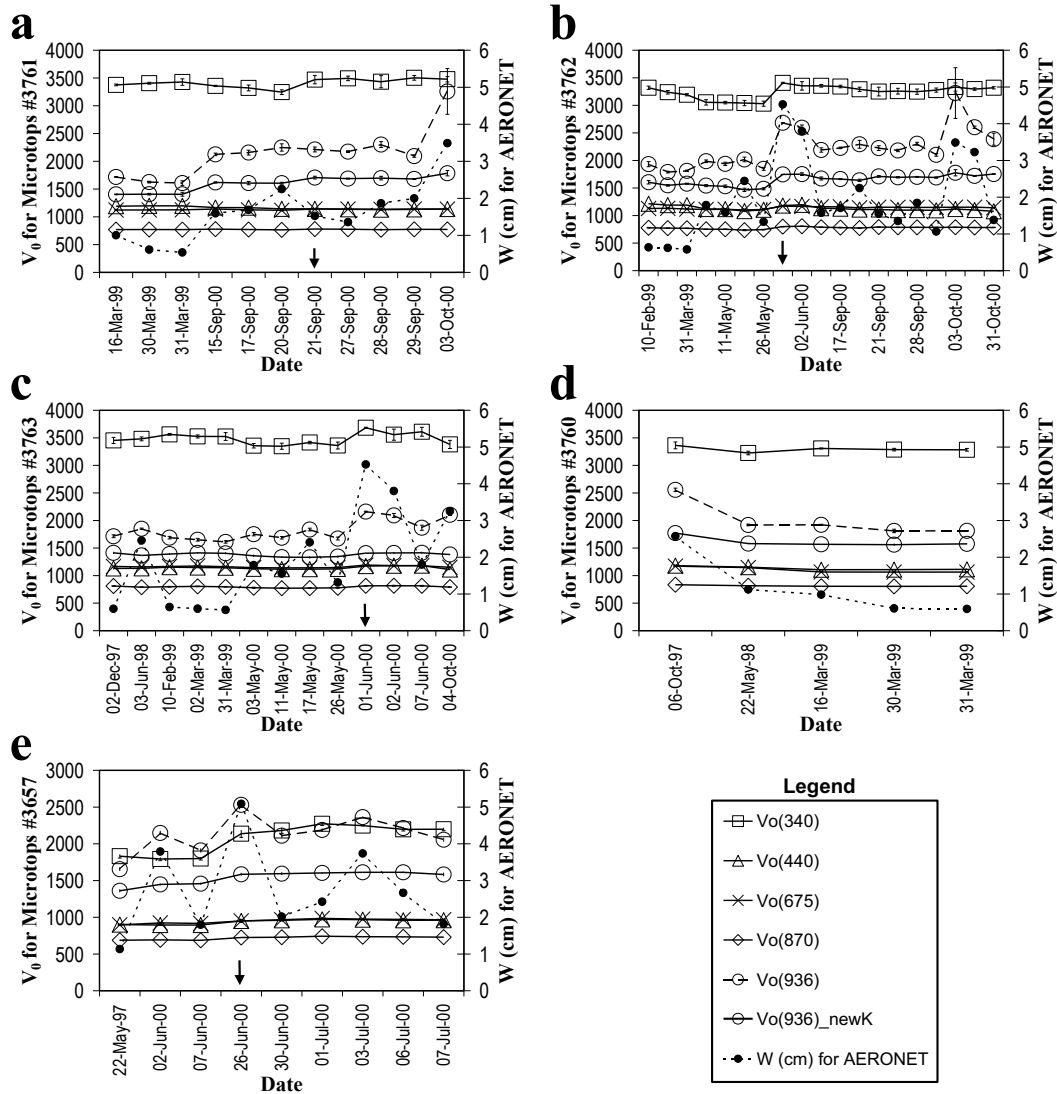
$$\ln(V_\lambda) = \ln(V_{0\lambda} D^{-2}) - \tau_\lambda M$$

Or

Transfer calibration from a Langley-calibrated Instrument

$$\frac{V_\lambda}{V'_\lambda} = \frac{V_{0\lambda}}{V'_{0\lambda}}$$

# Transfer Calibration of five Microtops sun-photometers against AERONET at NASA/GSFC

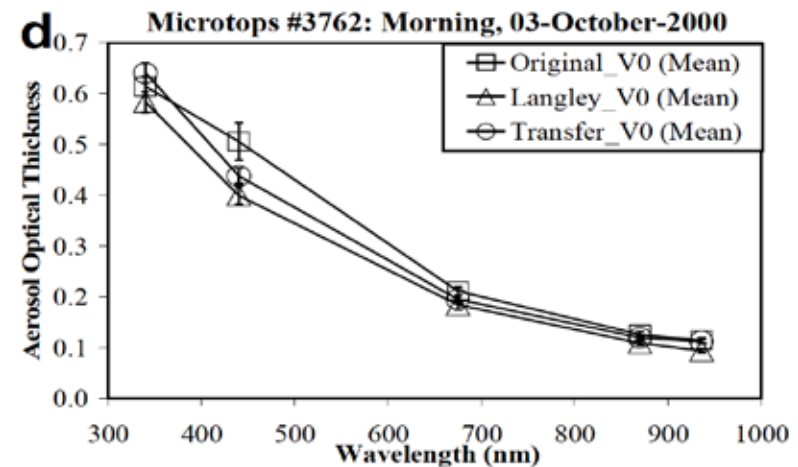
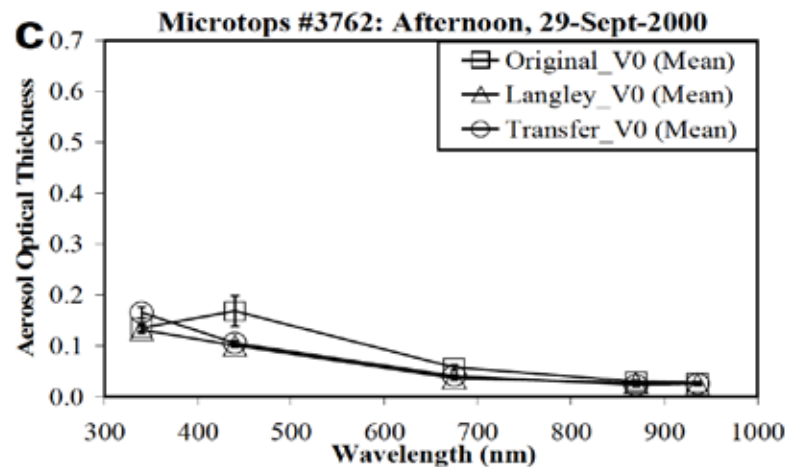
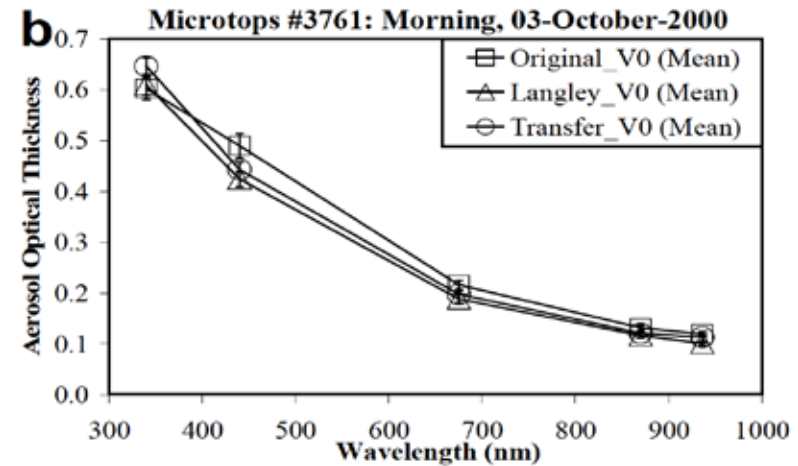
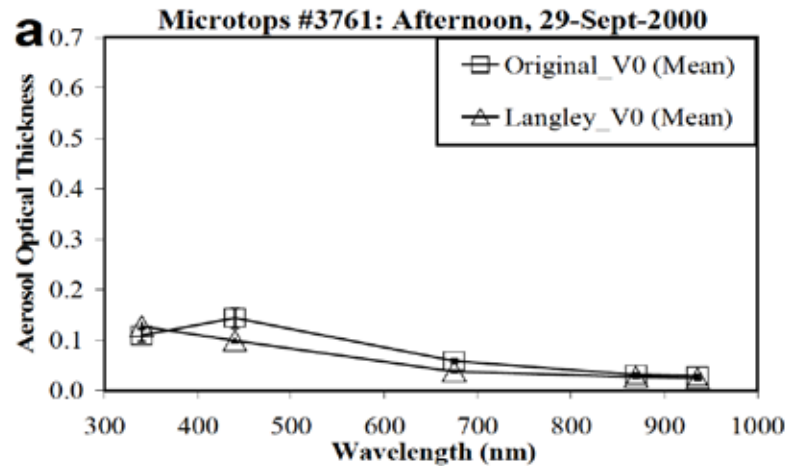


## Experiences

- Proper calibration takes a long time
- Pre- and Post-deployment calibration always required
- Uncertainty persists (why do the  $V_0$ s vary over time?)

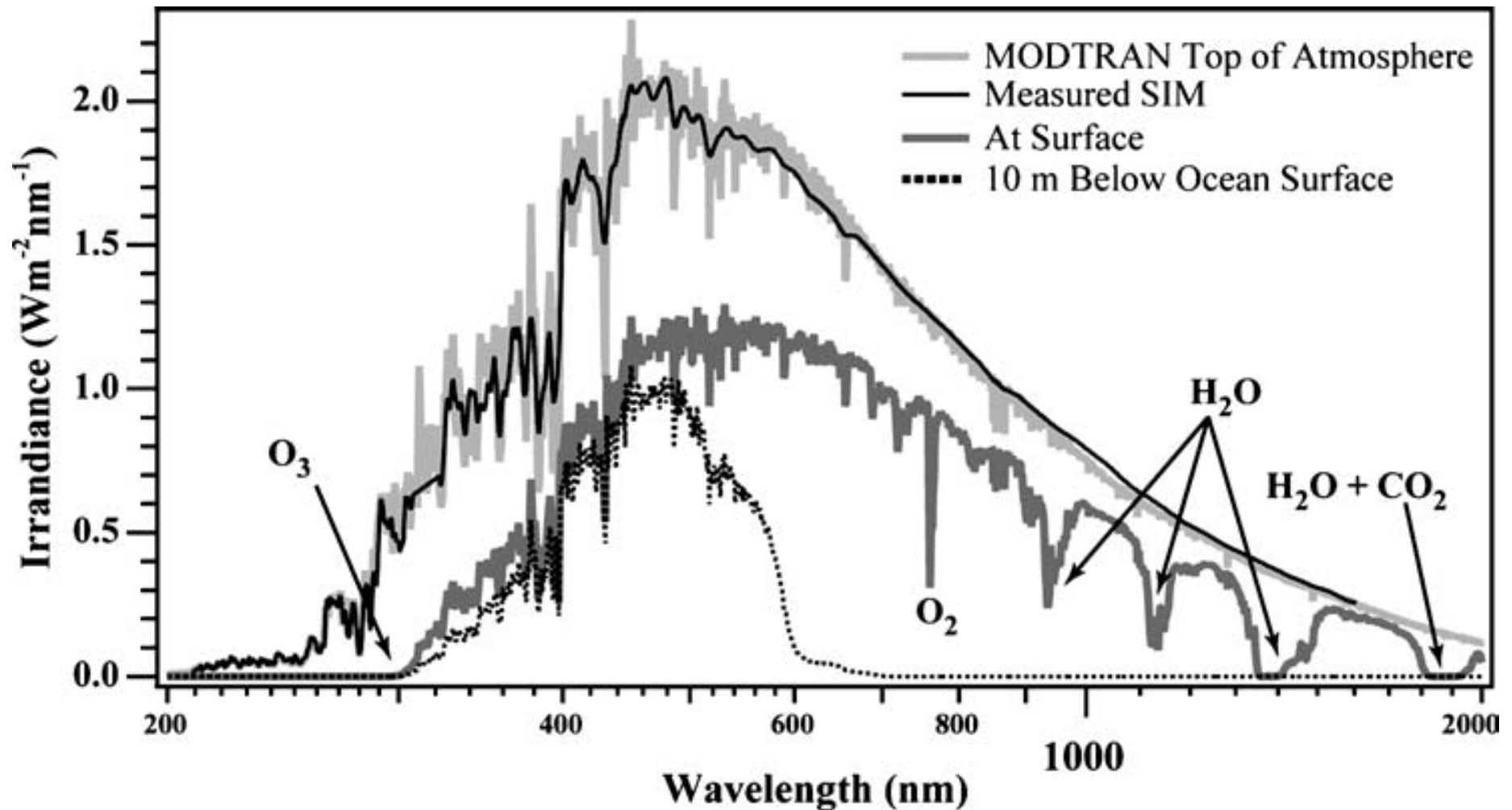
Ichoku et al., 2002, JGR, Microtops

# AOT values can differ significantly depending on calibration method



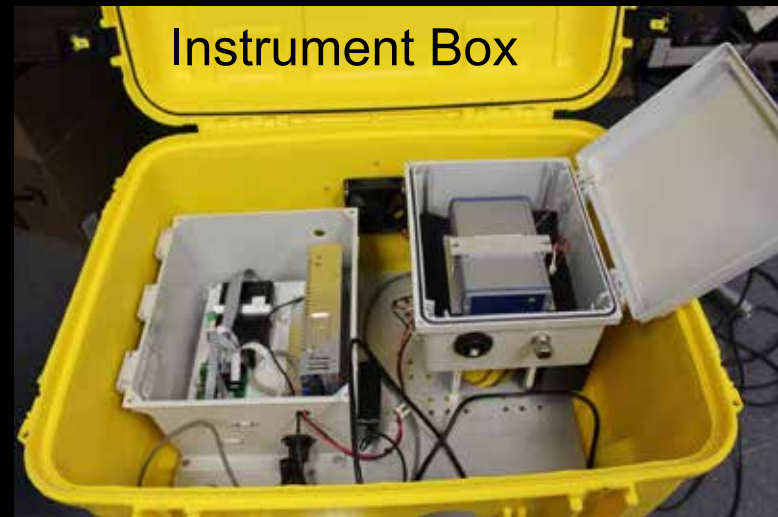
Ichoku et al., 2002, JGR, Microtops

# TOA-measured SSI seems more realistic than modeled



Harder et al., 2005, Solar Physics

# Pandora Spectrometer for Ground-based RS of Trace Gases



Herman et al., 2015, AMT paper on Pandora (p 3409):

The laboratory-calibrated Pandora TCO retrieval algorithm uses an external solar reference spectrum derived from a combination of the Kurucz spectrum (wavelength resolution  $\lambda/\Delta\lambda = 500\,000$ ) radiometrically normalized to the lower-resolution shuttle Atlas-3 SUSIM spectrum (Van Hoosier, 1996; Bernhard et al., 2004).

Herman et al., 2015, AMT paper on Pandora (p 3409):

The use of a well-calibrated top-of-the-atmosphere spectrum convolved with the laboratory-measured spectrometer slit function derived for each pixel permits derivation of ozone amounts without resorting to either a Langley calibration approach or calibration transfer from a standard instrument. The core slit function is known to within 1%, which propagates into an ozone error of less than 1%.

Smirnov, 2018, personal communication:

This statement is correct, but only if we are sure that SSI is known with an uncertainty of less than 0.5%.

Coddington et al., 2014, BAMS paper on Solar Irradiance:

Table I. Measurement requirements established for the TSIS TIM and SIM instruments that are driven by the need to understand Earth's climate response to solar variability, for separating natural from anthropogenic climate forcing effects, and for the monitoring and interpretation of the variability in wavelength-dependent processes induced by changes in Earth's surface and atmosphere.

Parameter	TSI CDR requirement	SSI CDR requirement
Absolute accuracy	0.01%	0.2%
Stability	0.001% yr <sup>-1</sup>	0.05% yr <sup>-1</sup> ( $\lambda < 400$ nm)
		0.01% yr <sup>-1</sup> ( $\lambda > 400$ nm)
Relative precision	0.001%	0.01%

**Take Home Message:** If SSI measurements from TSIS and future missions meet these requirements, they should be seriously considered for calibration of Sun-pointing ground-based instruments

# Acknowledgements

The TSIS-1 Project

The AERONET Project

The Pandora Global Network (PGN) Project

## References

- Coddington, O., Lean, J.L., Pilewskie, P., Snow, M. and Lindholm, D., 2016. A solar irradiance climate data record. *Bulletin of the American Meteorological Society*, 97(7), pp.1265-1282.
- Dubovik, O., Holben, B., Eck, T.F., Smirnov, A., Kaufman, Y.J., King, M.D., Tanré, D. and Slutsker, I., 2002. Variability of absorption and optical properties of key aerosol types observed in worldwide locations. *Journal of the atmospheric sciences*, 59(3), pp.590-608.
- Dutton, E.G., Reddy, P., Ryan, S. and DeLuisi, J.J., 1994. Features and effects of aerosol optical depth observed at Mauna Loa, Hawaii: 1982–1992. *Journal of Geophysical Research: Atmospheres*, 99(D4), pp.8295-8306.
- Harder, J., Lawrence, G., Fontenla, J., Rottman, G. and Woods, T., 2005. The spectral irradiance monitor: scientific requirements, instrument design, and operation modes. In *The Solar Radiation and Climate Experiment (SORCE)* (pp. 141-167). Springer, New York, NY.
- Herman, J., Evans, R., Cede, A., Abuhassan, N., Petropavlovskikh, I. and McConville, G., 2015. Comparison of ozone retrievals from the Pandora spectrometer system and Dobson spectrophotometer in Boulder, Colorado. *Atmospheric Measurement Techniques*, 8(8), p.3407.
- Ichoku, C., Levy, R., Kaufman, Y.J., Remer, L.A., Li, R.R., Martins, V.J., Holben, B.N., Abuhassan, N., Slutsker, I., Eck, T.F. and Pietras, C., 2002. Analysis of the performance characteristics of the five-channel Microtops II Sun photometer for measuring aerosol optical thickness and precipitable water vapor. *Journal of Geophysical Research: Atmospheres*, 107(D13).
- Petrenko, M. and Ichoku, C., 2013. Coherent uncertainty analysis of aerosol measurements from multiple satellite sensors. *Atmospheric Chemistry & Physics*, 13, pp.6777-6805.
- Petrenko, M., Ichoku, C. and Leptoukh, G., 2012. Multi-sensor aerosol products sampling system (MAPSS). *Atmospheric Measurement Techniques*, 5(5), p.913.
- Sayer A. M., N. C. Hsu, C. Bettenhausen, J. Lee, J. Redemann, B. Schmid, and Y. Shinozuka (2016), Extending “Deep Blue” aerosol retrieval coverage to cases of absorbing aerosols above clouds: Sensitivity analysis and first case studies, *J. Geophys. Res. Atmos.*, 121, 4830–4854, doi:10.1002/2015JD024729.
- Smirnov, A., Petrenko, M., Ichoku, C. and Holben, B.N., 2017, October. Maritime Aerosol Network optical depth measurements and comparison with satellite retrievals from various different sensors. In *Remote Sensing of Clouds and the Atmosphere XXII* (Vol. 10424, p. 1042402). International Society for Optics and Photonics.